Sulaimani Journal for Pure and Applied Sciences Vol. 28 Issue 1 (2026) 1-17.

Journal homepage https://sjpas.univsul.edu.iq
Sulaimani Journal for Pure and Applied Sciences
ISSN:1812-4100

Original Article

Synthesis and Computational Studies of Divalent Nickle, Zinc, Cadmium, and Mercury Complexes with 5-(Benzoyl methyl) - 1,3,4 – Oxadiazole -2- Thione Ligand

Bayan Faiq *

Department of Chemistry, College of Science, Salahaddin University, Erbil, Kurdistan Region, Iraq.

ARTICLE INFO

Article History:
Received: 16/11/2025
Revised: 21/12/2025
Accepted: 20/1/2026
Published online: 25/06/2026

Key Words:
Oxadiazole Complexes
Spectroscopic Study
Antioxidant
Computational Studies
Synthesis

ABSTRACT

The overall formula $[M(L)_2]$ Complexes, where $M=Ni^{+2}$, Zn^{+2}, Cd^{+2} and Hg^{+2}; Where LH = {5-benzoyl methyl - 1,3,4- oxadiazole -2-thione} were prepared and characterized on the bases of CHNS analysis, to IR, UV-Vis, magnetic susceptibility, antioxidant assays and conductivity measurements, and NMR (^1H, ^{13}C) techniques, along with DFT, NBO, and MEP studies. Confirming based on CHNS and physical data measurements and computational studies of prepared complexes. All complexes exhibited non-electrolytic behavior and distorted tetrahedral structures, except for the Ni complex, which was a distorted square planar. Notably, the Zn (II) complex demonstrated the highest antioxidant activity (100%) due to effective hydrogen atom donation, while the activities of Ni (II) and Cd (II) complexes decreased due to instability. DFT and NBO analyses revealed significant charge transfer in the Zn and Cd complexes, with the Cd complex showing a greater affinity for sulfur donors. Additionally, the Cd complex displayed a smaller energy gap, indicating lower stability compared to the Zn complex.

1. Introduction

Compound 1,3,4-oxadiazole-2-thione belongs to a class of heterocyclic compounds with five members. It's a similar furan structure with the replacement of (2) carbon methene groups (–CH=) in the position (3 and 4) by two nitrogen atoms (Bala et al., 2014). Oxadiazoles exhibit unique characteristics linked to (Thiol ↔ Thione) tautomerism (Figure 1); thione (R1R2C=N-S) and a thiol (R1R2C-NH-SH) exist in balance between them, considerably influenced by medium PH or solvent, environmental conditions (Singh et al., 2010; Dilmaghani & Ghezelbash, 2016). Silver, copper, and zinc complexes with oxadiazole support adaptability of the ligands validating the integrity and bonding of their structure and properties determined by spectroscopy tool (Kazi, 2011).

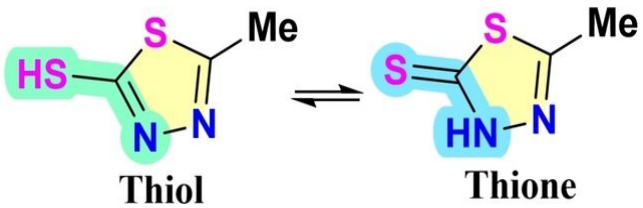

Figure 1. (Thiol ↔ Thione) tautomerism.

1,3,4-oxadiazole-2-thione compound has important medical care and synthetic chemistry owing to multipurpose physiological functions and applications. Recent studies have been discovered that 1,3,4-oxadiazole-2-thione utilized for various

* Corresponding author.
E-mail address: bayan.faiq@su.edu.krd (B. Faiq)

applications, particularly in the field of medicinal chemistry as it functions as significant structure for the plan of new anti-infective agents (Al-Wahaibi et al., 2021). This compound displays a series of biological functions, which include germicidal, prophylactic , antiviral, antifungal, and anti-inflammatory properties. (Akram et al., 2018; Husain & Ajmal, 2009). For example, 1,3,4-oxadiazole-2-thione has been shown to have significant antibacterial traits, effectively combating resistant strains of a variety of diseases. (Akram et al., 2018) ;(Li et al., 2011). Furthermore, drug design studies have brought out its potential as a urease inhibitor, its showing relevance in treating Influence of sickness by this enzyme, kidney stones (Akram et al., 2018). The derivatives of 1,3,4-oxadiazole-2-thione pharmacological activity stretches into other medical specialties, part including the treatment of cancer, where they have shown anti-proliferative action against cancer cell lines (Abdelrehim, 2021). The chemical drug design linked with nickel complexes, and oxadiazole ligands potent biological activities, and cell-killing effects especially palladium and platinum complexes (Geyl et al., 2022). Moreover, they play an essential role in the synthesis of composite materials and polymers applicable in optoelectronic devices due to their favorable luminescent and electronic properties (Tzanetos & Kallitsis, 2005).

Preparation and theoretical (DFT) studies of nickel complex with oxadiazole ligand illustrates the electronic structure and properties of nickel metal complexes linked with the oxadiazole ligand (Nkungli et al., 2015). In this paper, the complexes of Ni (II), Cd (II), Zn (II) and Hg (II) with 5-benzoyl methyl 1,3,4-oxadiazole-2-thione were prepared experimentally. Therefore, the novelty of this paper were represented by synthesis and computational studies of divalent Nickle, Zinc, Cadmium, and Mercury complexes with 5-(benzoyl methyl) - 1,3,4 – oxadiazole -2- thione ligand and identified by means of CHNS analysis, ^{1}HNMR, ^{13}CNMR, IR, Uv-Visb., conductivity, magnetic susceptibility, antioxidant, DFT, MEP and NBO studying.

2. Synthesis

2.1. Experimental & Materials

The compounds $NiCl_2{\cdot}6H_2O$, $ZnCl_2$, $CdCl_2{\cdot}2H_2O$, and $HgCl_2$ were purchased from Sigma Aldrich. The chemical reagents, including CS_2, ethanol (99.9%), and DMSO (99.8%), were supplied by Fluka, Merck, and Sharlau, respectively, and were used in their unpurified state.

Melting points were recorded using the capillary method with an Electrothermal IA 9000 melting point apparatus (England). The ^{1}H, ^{13}C NMR, and elemental (CHNS) analyses were performed at the Photon Center, University of Baghdad. UV-Vis spectra were obtained using a SHIMADZU UV-1900i Spectrophotometer over a wavelength range of 200-1000 nm. Infrared (IR) spectra were acquired between 400 and 4000 cm^{-1} using a Thermo Mattson 300 FT-IR spectrophotometer. The conductivities of the prepared coordination compounds in DMSO were measured with a JENWAY 4520 Electrical Conductivity Meter.

2.2. Preparation of 5-benzoyl methyl-1, 3, 4-oxadiazol-2-thione

To a solution of potassium hydroxide (0.01mol, 0.56g) in absolute ethanol (20 ml) was added benzoyl methyl acid hydrazide (0.01 mol, 1.78g), followed by CS_2(0.02 mol, 1.52g). The reflux of mixture was gone on for 16 hours till the release of H_2S gas ceased (Fig. 2). The solvent was concentrated and treated with diluted HCl acid (1:1). The obtained solid was filtered off, washed with distilled water, dried under vacuum, and recrystallized from ethanol (Aydoğan et al., 2022).

2.3. Preparation of metal complexes

A water-based solution of (0.01 mol) of a relevant metal salt ($NiCl_2.6H_2O$, $ZnCl_2$, $CdCl_2.2H_2O$ and $HgCl_2$) was added to water-based solution of 5-benzoylmethyl-1,3,4-oxadiazole-2-thione (0.02 mol)

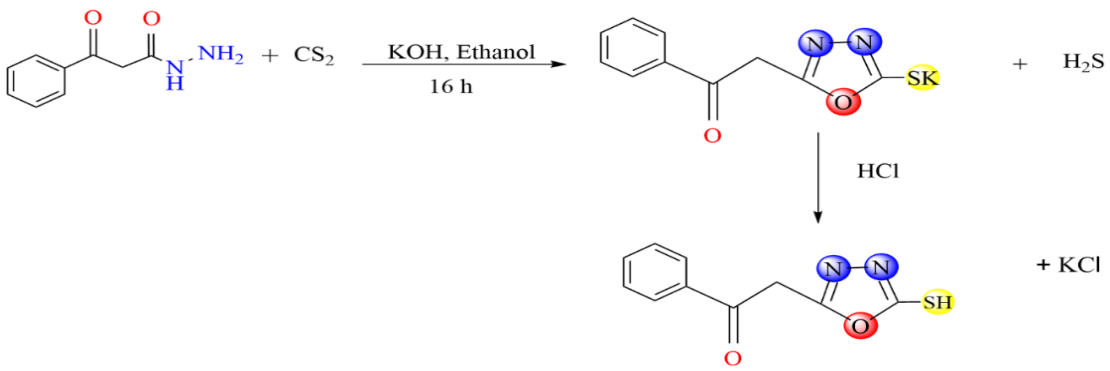

Figure 2. Chemical Reaction for preparation (5-benzoyl methyl-1, 3, 4-oxadiazol-2-thione).

and potassium hydroxide (0.02 mol). At once, precipitates of various colors were produced at room temperature. The formed solids were separated by a filter, washed with distilled water, and dried at 50°C

3. Results and Discussion

3.1. Elemental Analysis

The chemical and physical properties of the prepared ligand (LH) and complexes are illustrating in Table 1. These metal complexes were synthesized using Ni (II), Zn (II), Cd (II) and Hg (II) salts in coordination with 5-benzoylmethyl-1,3,4-oxadiazole-2-thione ligand. The measurements of calculated (CHNS)analysis were acceptable with experimental percentages, which consisted of complexes in small acceptable discrepancies within the permissible range (±0.4 %). This consistency suggests their stoichiometric settings. The correspondence between calculated data and the results obtained from laboratory confirms purity of prepared compounds.

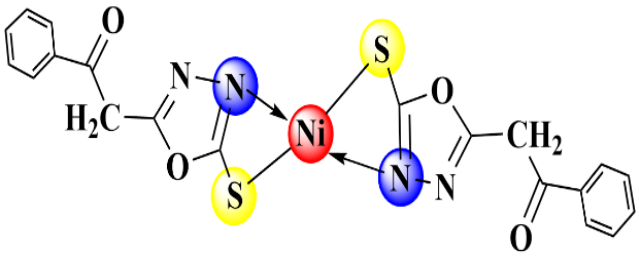

Suggested Structure of distorted square planner Ni complex.

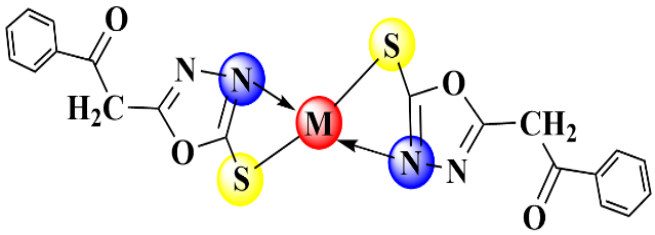

Suggested Structure of distorted tetrahedral M= (Zn (II), Cd (II) and Hg (II) complex.

3.2. Infrared Spectra Studies

Infrared spectra of the free ligand LH display characteristic υ (N-H) and υ (S-H) bands stretching at (3120) cm^{-1} and (2567) cm^{-1} respectively. These bands are completely absent from the spectra of all four metal complexes. (Aboraia et al., 2006) confirms deportation of both functional groups and their subsequent coordination to the metal center, forming (M-N) and (M-S) bonds. (Nakamoto, 2009). The mode of coordination of the ligand could be distinguished by the analysis of thioamide band (Fig. 3). The directions of the shifts of all bands in the spectra of the similar complexes. This fact clearly indicates that the bonding model must be the same in all complexes. The LH containing thioamide group rise to four thioamide bands in the infrared spectrum. Thioamide band(I) appeared at (1544) cm^{-1}, band (II) at (1487) cm^{-1}, band (III) at (925) cm^{-1}) and band (IV) at (748) cm-1 (Pandey et al., 2010). Thioamide Band I has major contribution from (δ(N-H) + υ (C-N), this band undergoes a consistent positive shift from (1544) cm^{-1} in the free ligand to higher wavenumbers in the complexes (1554-1581) cm^{-1}.The increase in the υ (C-N) frequency is a direct

Table 1: Elemental analysis (CHNS) analysis and other physical properties attributes of the ligand and its complexes.

Compounds	M. Wt. g/mol	C	H	N	S	m.p (°C)	color	%Yield
			(Cal.)	Found				
$C_{10}H_8O_2N_2S$		(53.54)	(3.59)	(12.49)	(14.29)	226.3-227	Yellow	64.45%
LH	220.204	54.39	3.25	12.17	14.15			
$[Ni(C_{10}H_7O_2N_2S)_2]$		(47.54)	(2.78)	(11.08)	(12.69)	>295 d	Pale Yellow Olive	87.40%
$[Ni(L)_2]$	497.082	47.26	2.53	10.86	11.97			
$[Zn(C_{10}H_7O_2N_2S)_2]$		(46.92)	(2.75)	(10.94)	(12.52)	> 242 d	Light yellow	71.70%
$[Zn(L)_2]$	503.782	46.38	2.63	10.76	11.87			
$[Cd(C_{10}H_7O_2N_2S)_2]$		(42.97)	(2.52)	(10.02)	(11.47)	> 265 d	Lemon yellow	89.55%
$[Cd(L)_2]$	550.803	42.83	2.41	9.94	10.98			
$[Hg(C_{10}H_7O_2N_2S)_2]$		(37.11)	(2.17)	(8.65)	(9.91)	> 239 d	Orange	61.06%
$[Hg(L)_2]$	638.982	37.02	2.11	8.52	9.79			

consequence of nitrogen atom in coordination (Dani et al., 2014). Band (II) has contribution from (δ(C-H) + υ(C-S) + υ (C- N) in free ligand show band at (1487) cm^{-1} and no significant change (1492-1483) cm^{-1}, after complexations (Aydogan et al., 2002). Band (III) mixed υ (C-N) + υ (C-S) show band at (925) cm^{-1} showing a slight positive shift for Ni, Zn, and Cd complexes (952) cm^{-1} (Bhartya et al., 2015). Band (IV) has contribution from predominant of υ (C-S) that show band (748) cm^{-1}. While band (IV) is disappeared after complexations confirming that the metal ion is linked to S atom (Pandey et al., 2010; Shaker, 2010; Saaid et al., 2018). The stretching vibrations of (C-O) appear about (1178 cm^{-1} and 1068cm^{-1}) with no significant change after complexations, while the band (C-O-C) observed at (750) cm^{-1} remains the same in ligand and all complexes (Aboraia et al., 2006). The whole complexes show a weak band in a very narrow ranges (551-554) cm^{-1}, assigned to the (M-N) stretching vibration and a second set of new bands appears between (418-450) cm^{-1}, assigned to (M-S) stretches (Figs. 4 and 5) (Bharty et al., 2012; Bharty et al., 2015; Sundaresan et al., 2022). The electronic transitions and their assignment are listed in Table 2.

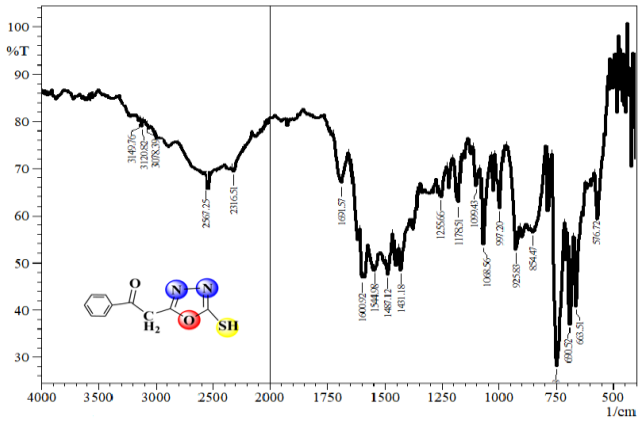

Figure 3. I.R Spectrum of oxadiazole ligand.

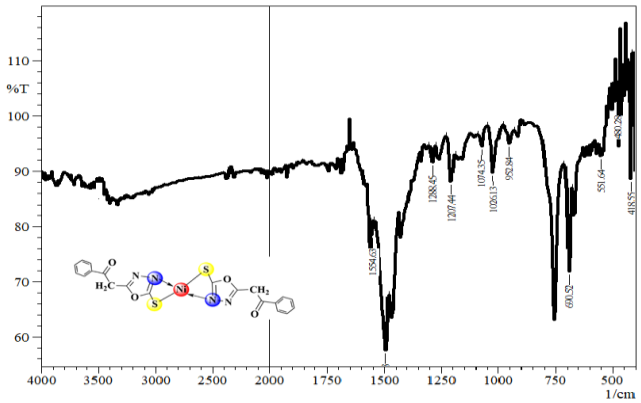

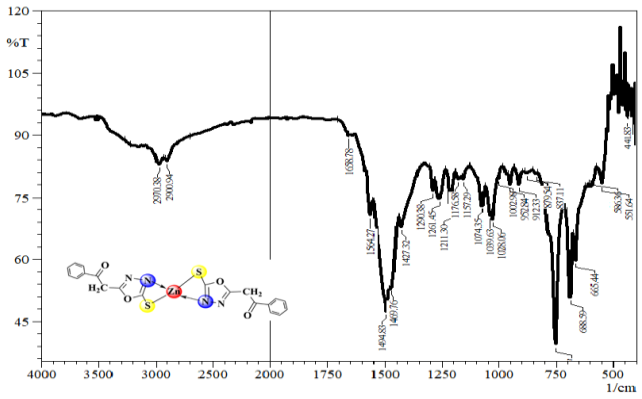

Figure 4. I.R Spectra of Ni (II), and Zn (II) complexes.

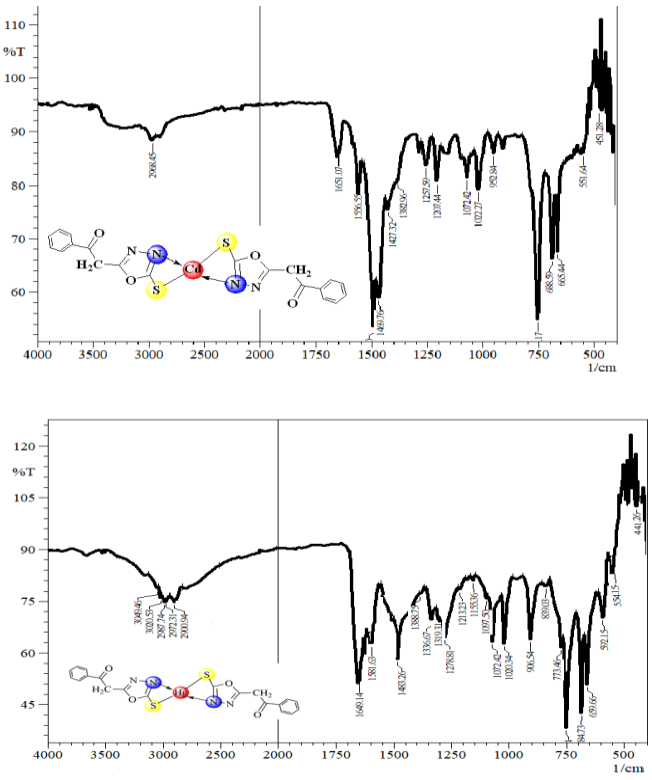

Figure 5. I.R Spectra of Cd (II), and Hg (II) complexes.

3.3. Electronic transition spectra

ligand-based π→π* and n→π* transitions all affect their Uv-Visb. Spectra (Fig. 6). These spectrum signals are highly sensitive indicators of metal-ligand binding, analytic geometry, and ligand electronic effects. At around 260 nm, ligand-based π→π*: agrees with ligand and aromatic π orbitals. Non-bonding n→π* (~272 nm): attributable to lone pairs of heteroatoms, namely nitrogen, that participate in n→π* transitions. These transitions, which take place between (272) and (269) nm, include the movement of non-bonding electrons on heteroatoms (like nitrogen) to π* orbitals. Zinc (II), cadmium (II), and mercury (II) complexes are well-known (d^{10} configuration). Accordingly, these complexes usually hide d-d transitions in visible regions owing to the unavailability d electrons for transitions. Alternatively, their electronic spectra chiefly feature charge transfers bands. For example, Zn^{+2}, Cd^{+2}, and Hg^{+2} complexes studies show no absorption bands in extent of (380-1000) nm excerpt to d-d transitions, underlining the absence of these transitions and confirm the diamagnetism nature (Dhaveethu et al., 2013; Mohammed et al., 2018). Substantial absorption bands were viewed at around (28169) cm^{-1} for $[Hg(L)_2]$ complex, (28248) cm^{-1} for $[Cd(L)_2]$ complex, (28336) cm^{-1} for $[Zn\ (L)_2]$ complex, which are ascribed to ligand-to-metal charge transfer transitions instead of d-d transitions (Mohammed et al., 2018). Confirming based on CHNS and other physical measurement, tetrahedral geometry is suggested for these complexes. According to the above-mentioned physical measurements while $[Ni(L)_2]$ complex reflected bonds at (20250) cm^{-1} and (15505) cm^{-1}, respectively segment to d-d transitions of the type $^1A_1g \rightarrow {}^1A_2g$ and $^1A_1g \rightarrow {}^1B_1g$ as showed in Table 3. These transitions suggest the square planner geometries of the ligand around Ni metal in this complex (Demir and Pekacar, 2005). Furthermore, the low value of molar conductivity (2.2-5.3) $\Omega^{-1}cm^2$ mol^{-1} confirms that the complexes are non-electrolyte.

3.4. ^{1}H-NMR &13CNMR Spectra

Typically, the ^{1}H NMR spectrum of 1,3,4-oxadiazole-2-thione sections of characteristic signals that help identify the hydrogen surrounding within the compound bonded protons to carbon atoms next to the oxadiazole ring and groups have an impact on in the range of 7.0 to 7.6 ppm (Fig. 7), suggestive of aromatic hydrogens (Prabhu et al., 2012; Tang et al., 2015).

Table 2: Selected IR bands of the ligand and its complexes.

Compounds	υ(NH)	υ (SH)	Thioamide Band (I)	Thioamide Band (II)	Thioamide Band (III)	Thioamide Band (IV)	υ(M-N)	υ(M-S)
LH	3120	2567	1544	1487	925	748	------	-----
$[Ni(L)_2]$	------	------	1554	1494	952	-------	551	418
$[Zn(L)_2]$	-------	------	1564	1494	952	-------	551	441
$[Cd(L)_2]$	-------	------	1556	1492	952	-------	551	450
$[Hg(L)_2]$	-------	------	1581	1483	906	-------	554	441

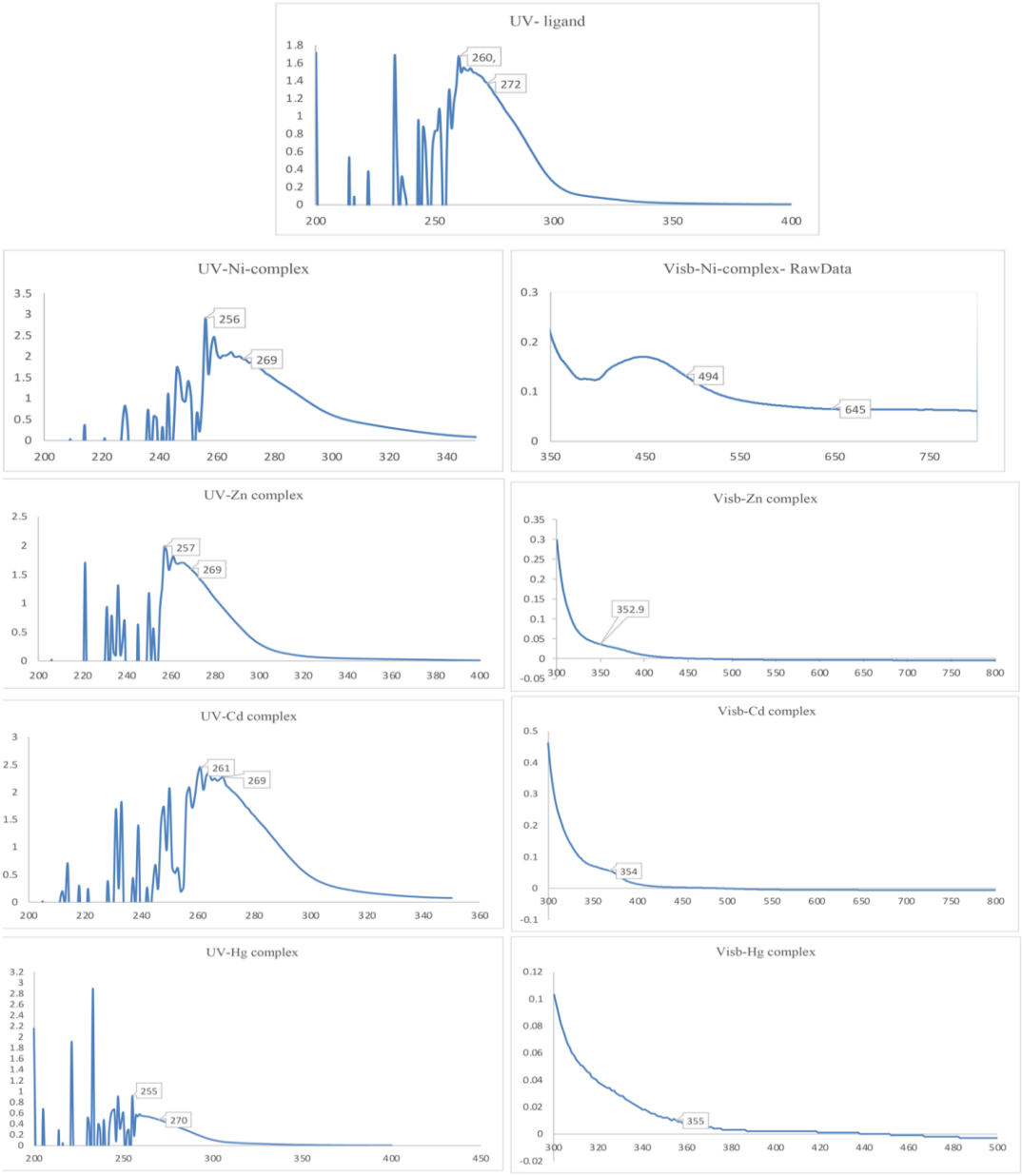

Figure 6. UV- Visible Spectra for oxadiazole ligand and complexes.

Table 3: Uv-vis, magnetic susceptibility and conductivity measurements.

Complexes	Absorption cm-1	Absorption nm	Assignment	Magnetic susceptibility	ΛM ($\Omega^{-1}cm^2$ mol^{-1}) in DMSO
	38461	260	π⟶ π*		
Ligand (LH)	36764	272	n⟶ π*	-------	1.05
	38461	256	π⟶ π*		
	36764	269	n⟶ π*		
[NiL_2]	26954	371	C.T	Diamagnetic	2.2
	20250	494	$^1A_1g \rightarrow {}^1A_2g$		
	15505	645	$^1A_1g \rightarrow {}^1B_2g$		
	38910	257	π⟶ π*		
[ZnL_2]	37174	269	n⟶ π*	Diamagnetic	2.4
	28336	353	C.T		
	38314	261	π⟶ π*		
[CdL_2]	37174	269	n⟶ π*	Diamagnetic	3.6
	28248	354	C.T		
	39215	255	π⟶ π*		
[HgL_2]	37037	270	n⟶ π*	Diamagnetic	5.3
	28169	355	C.T		

Furthermore, protons on the (S-H) group (if tautomerization results in its prevalence) may display chemical shifts reflecting their individuality electronic surroundings, though they are infrequently observed due to quick exchange with solvent protons. The aromatic phenyl protons show singlets between ^{1}H NMR {300 MHz, DMSO-d_6} δ 7.66 ppm (d, J = 7.6 Hz, 2H), 7.40 ppm (t, J = 7.5 Hz, 2H), 7.30 ppm (t, J = 7.3 Hz, 1H) belongs to phenyl group, 5.87 ppm (s,1H) belongs (S-H) group, 4.37 ppm (s, 2H) belongs to the CH_2 group. In all complexes ^{1}H NMR {300-MHz, DMSO-d_6} δ (6.98-7.95) ppm (m, 10H), belongs to phenyl groups, (4.35-4.41 ppm) (s, 4H) belongs to the CH_2 group and S-H signal disappeared confirming that the metal ion is linked to S atom (Figs. 8 and 9).

The ^{13}C NMR spectrum supports this structural analysis by revealing section corresponding to the carbon atoms existing in 1,3,4-oxadiazole heterocyclic ring (Fig. 7). The aromatic phenyl ring carbon showed δ at (125.47, 128.50, 129.09) ppm, δ at (129.50, 131.18) return to C5 and C2, (δ (144.10) ppm return to C10. The separate carbon signal at (161.67) ppm for the carbon atom (C-SH) engaged in the conformation of the heterocyclic structure (Prabhu et al., 2012) and near (192.2) ppm for the carbon atom which is belonged (C=O) group and chemical shift appeared at δ (34.10) ppm can be assigned to the (CH_2) group (Mikhailov et al 2019). This evidence shows the presence of the (SH) group that stabilizes the oxadiazole ring.

Table 4: Antioxidants Results for ligand and prepared complexes.

No.	Ligand and it`s Complexes	The percentage of ligand and its complexes that scavenge		
		20 µg /ml	40 µg/ml	60 µg/ml
1	Ligand (LH)	76	77	80
2	[NiL_2]	100	98	83
3	[ZnL_2]	100	100	100
4	[CdL2]	100	100	78
5	Ascorbic Acid (Vitamin C)	84	86	92

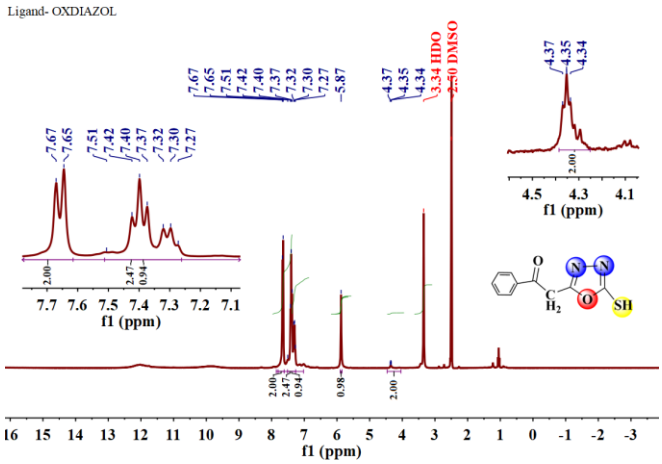

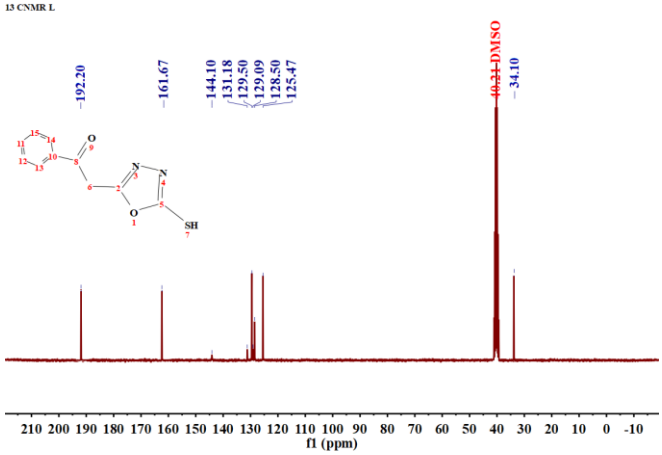

Figure 7. [1]HNMR &13CNMR for Oxadiazole ligand.

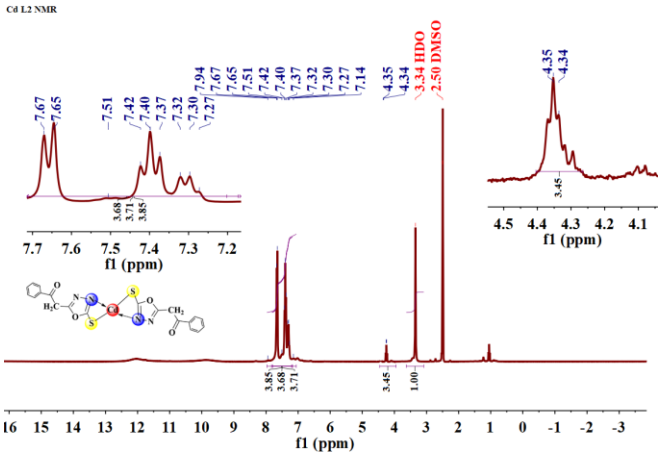

Figure 8. [1]HNMR spectra of Zn (II), and Cd (II) Complexes.

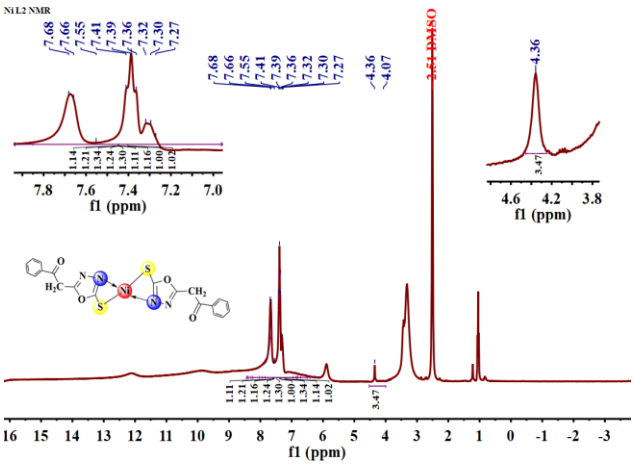

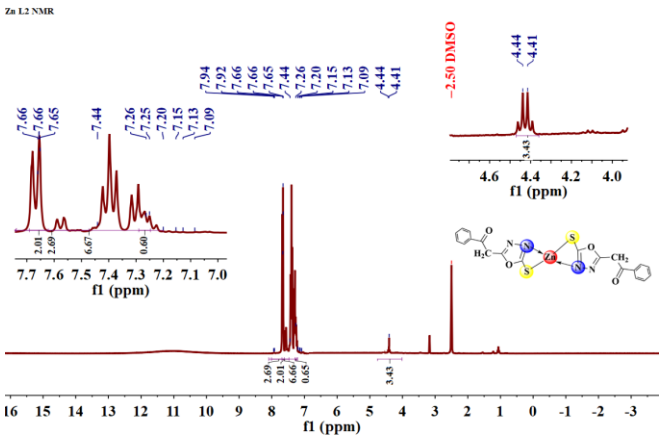

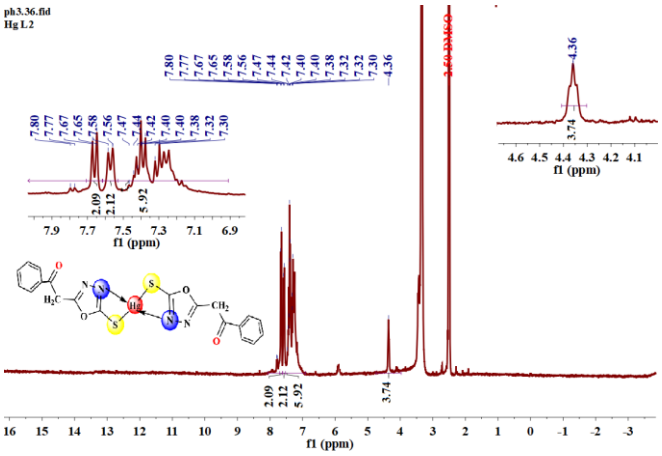

Figure 9. [1]HNMR of Ni (II), Hg (II) Complexes.

3.5. Antioxidant Studies for ligand and complexes

A very tiny amount of the ligand and it's divalent of {Ni, Zn and Cd} complexes were dissolved in some drops of dimethyl sulfoxide, to approach the needed (20µg/ml, 40µg/ml and 60µg/ml) micrograms per milliliter concentration by addition of ethanol. among all the prepared complexes note that Ni(II) and Cd(II) complexes start at (100%) antioxidant activity but they decrease to lower value due to instability, compared with Zn (II) complex was highest value (100%) of antioxidant activity across all concertation causing strong donating hydrogen atoms to neutralize free radical (DPPH) effects compared with Ascorbic Acid, while the ligand has lower value indicating Zn(II) complex was outperforms of (Vit. C). (Baliyan et al., 2022; Sundaresan et al., 2022; Silva et al., 2024).

4. Computational Studies of prepared ligand and complexes

4.1. DFT Studies (Optimized)

The GW9 Gaussian 16 program was employed to optimize the shape of the ligand and its metal complexes. The computations utilized the hybrid density functional theory (DFT) method B3LYP in conjunction with the 6-311G (d, p) basis set to optimize the molecular geometries (Tegegn et al., 2024). (FMOs - Frontier molecular orbitals), namely the highest in use molecular orbital and the lowest vacant molecular orbital. The compounds stability depends on LUMO value that is essential for evaluating the chemical response, the greater E-gap being approaching stability. The (DFT) studies applying diverse computational approaches and descriptive parameters. Thermodynamic steadiness can be estimated using (Gibbs free energy) values; nevertheless, molecular orbital {MO} and the electron density inquiries furnish a deeper comprehension of the electronic operations impacting molecular stability (AL-Nama et al., 2025).

The EHOMO and ELUMO values of oxadiazole ligand and its complexes (Zinc, Cadmium) are listed in Table 5. Both {EHOMO and ELUMO} are negative, illustrating the products stability. In addition, complexes with small E gap value were more reactive compared with high value E gap, while complex high value of E gap (ΔE) was more stable compared with another have low E gaps. In present studies [Zn complex] that have (0.31739 eV) is more stable than [Cd complex] that have (0.30288 eV) (Chaudhary et al., 2019; Tegegn et al., 2024).

Charge transfer interface within the LUMO-HOMO molecule is characterized by the forbidden energy gap (ΔE = ELUMO - EHOMO), as shown (Figs. 10- 12), and in Table 5.

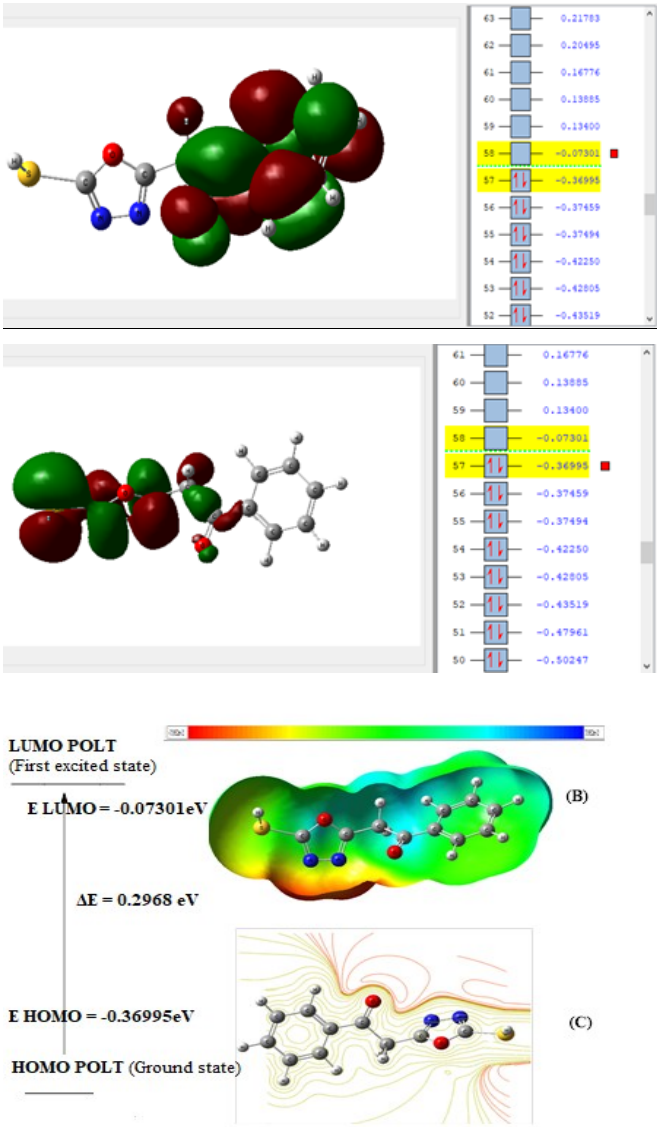

Figure 10. Surface Plot for HOMO and LUMO Orbitals for ligand.

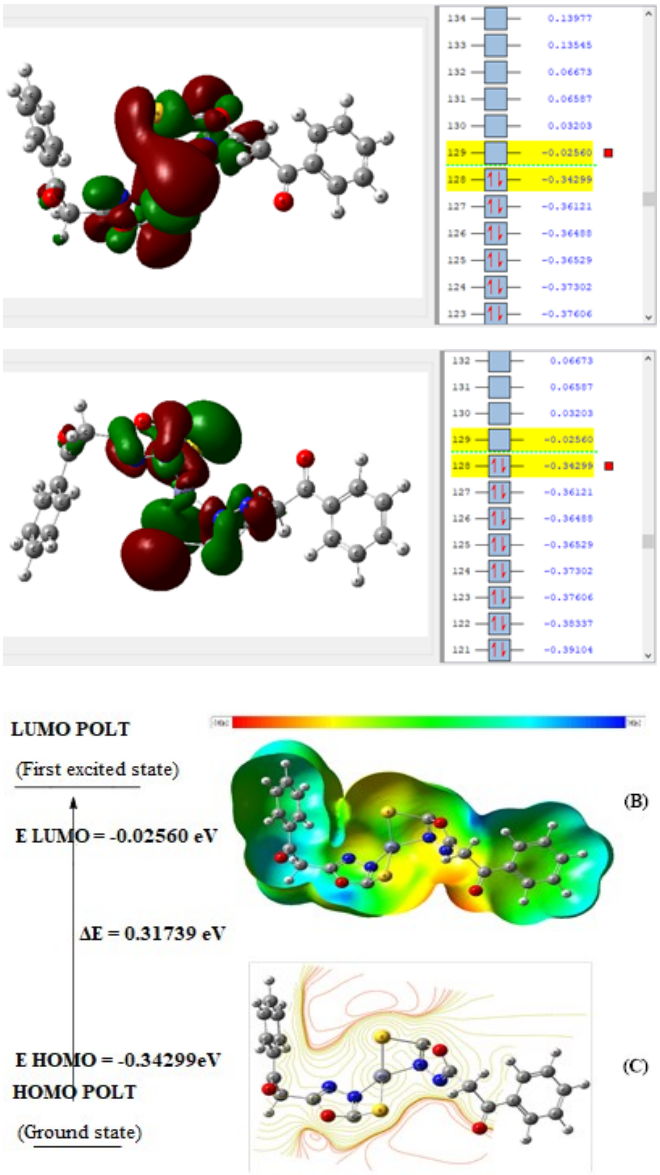

Figure 11. Surface Plot for HOMO and LUMO Orbitals for Zn complex.

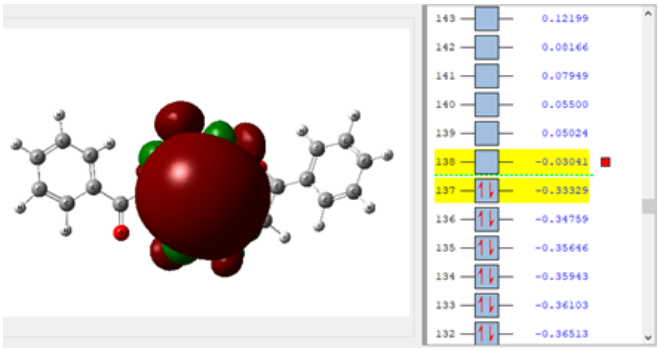

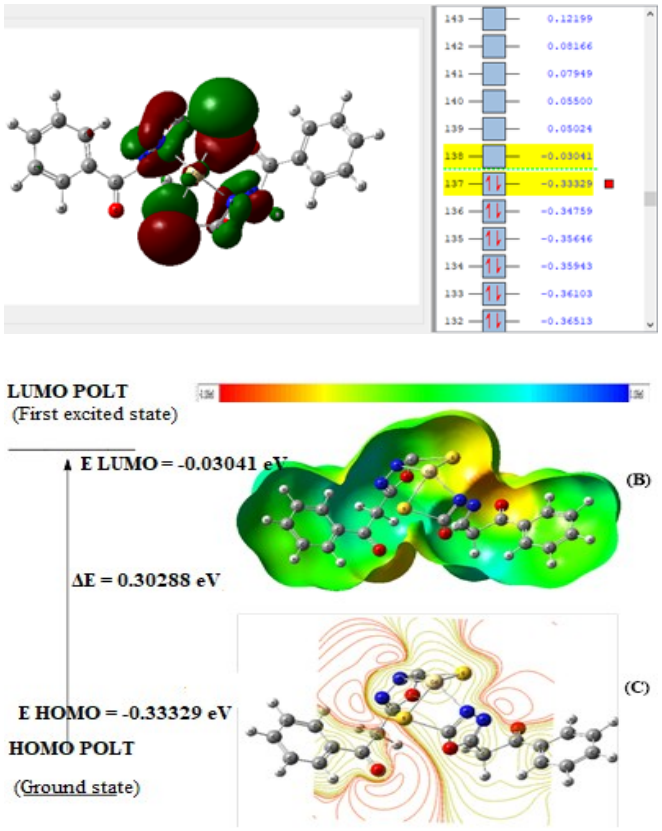

Figure 12. Surface Plot for HOMO and LUMO Orbitals for Cd Complex

4.2. Molecular Electrostatic Potential (MEP) Studies

Molecular Electrostatic Potential (MEP) is important Computing tool in rational drug design that illustrates the quantitative understanding of a molecule's electrostatic properties, which in turn dictates its interactions with biological targets. (MEP) helps researchers predict how a possible drug molecule will interact with a receptor or enzyme's active site, enabling the design of ligands with optimal recognition and binding. Furthermore, the (MEP) is topological analysis of molecular surfaces that offers a significant insight into electronegativity and partial charge distribution. This approach is very precise for forecasting intermolecular forces with biological models, specifically within the realm of charge-dipole, dipole-dipole, and quadrupole-dipole interaction. (MEP) represents an indicative molecular characteristic, dipole approximation, structure and Molecular polarity.

Table 5: EHOMO, ELUMO and some quantum chemistry characteristics for ligand and prepared complexes:

Parameters	Ligand	Zn-complex	Cd-complex	Main realization
E_{HOMO} (eV)	-0.3699	-0.3429	-0.3332	E_{HOMO} Signifies that after complexation, the molecule becomes more electron -rich and hence has a stronger grantor nature.
ELUMO (eV)	-0.0730	-0.0256	-0.3041	The Cd-complex has the lowest E_{LUMO}, sense it is more sloping to accept electrons. that cadmium, in this complex, is a better electron acceptor contrast to zinc.
ΔE (eV)	0.2968	0.3174	0.3029	A larger (E gap) regularly indicates more stability, because it's more difficult for the system to undergo transitions. The (Zn-complex) is more stable than (Cd-complex), which has a smaller (E gap).
IP (eV)	0.3699	0.3430	0.3333	(Cd-complex) has low ionization energy, **high** electron affinity It becomes simpler to remove an electron from the complex
EA (eV)	0.0730	0.0256	0.3041	The (Cd-complex) is more electrophilic having the highest electron affinity
χ(eV)	0.2214	0.1843	0.3187	(Cd-complex) has a stronger inclination to attract electrons towards itself (EN) relative to the (Zn-complex), showing the electronegativity of the complex. In this case, cadmium appears to have a greater appeal to the electrons in the system.
η(eV)	0.1484	0.1602	-0.0146	(Zn-complex) is perceived harder, **i**mplication it is more chemically stable. The (Cd-complex), has negative hardness, which is non-physical
σ (eV)-1	6.7364	6.2416	-68.6813	Hardness is the opposite of softness, negative softness is an anomalous and nonphysical outcome**,** which the author is responsible for the calculation
- ϱi (eV)	0.2214-	-0.1843	-0.3187	(ϱi = –χ) the negative softness {and possibly the negative hardness}

Moreover, they help identify lacking electrons (electrophilic) and (nucleophilic) electron-rich areas, which are the properties that are essential for chemical reactivity. MEP is commonly indicated by color: red corresponds to maximum electron density, blue indicates the areas, while green color indicates zone of nearly zero potential. (Derafa et al., 2024**;** Abd El-Nasser & Ismail, 2025).

The electrostatic potential constant lines illustrate electron density in the plane of the molecule according to counter plots. The yellowish-green portions typically are a sign of insufficient-electron sites, while red represents reinforcing electron-wealthy regions, specifically surrounding heteroatoms (Fig. 13). MEP (Molecular electrostatic potential) computations were carried out at (0.004 a.u.) for an electron density. The subsequent finding of contour plots and MEP denote that the oxadiazole ring demonstrates electron-donating properties and are capable of hydrogen bonding with biological target molecular (TARGET). Interpreting these electrostatic potentials are essential for computational chemistry at active sites, which form a simple rational drug design that develop stable and particular complexes (Faloye et al., 2025; Kurahatti et al., 2025).

4.3. Natural Bond Orbital (NBO) analysis Studies

Divalent of Zinc-Cadmium complexes compound with heterocyclic ligand (5-benzoyl methyl-1,3,4-oxadiazole 2-thione) nitrogen and sulfur-containing that carry out the role of worthwhile donator positions. The (NBO) analysis reveals a significant and strong trend of δ gift chelation, supported by a substantial overlap between completely full ligand molecular orbitals and metal empty orbitals (Kazi, 2011**;** Nkungli et al., 2015). The heterocyclic oxadiazole ring achieves stable electronic configurations in these two complexes which have an essential role in their stability and reactivity. The calculations confirm that divalent Zn complex was greater energy of stabilization compared to divalent Cd complex given its smaller size of Zn ion yielding

strong results of δ bonds (Singh et al., 2010; Bharty et al., 2015).

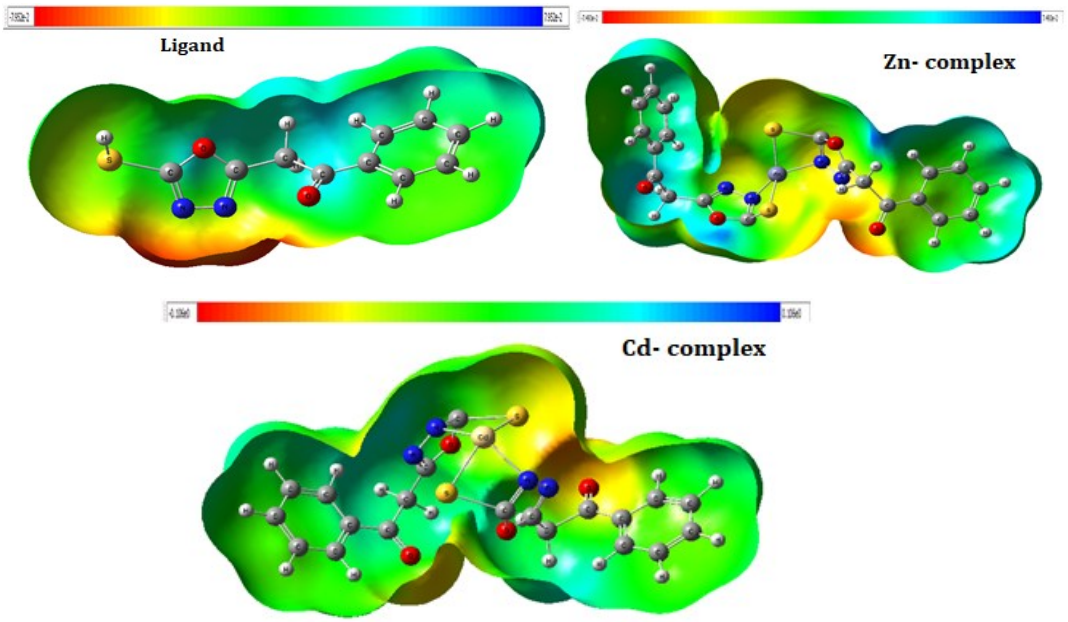

Figure 13. MEPS of Ligand and Zn, Cd complexes.

Positive charges are carried by both Zn and Cd (Zn: + 0.82, Cd: +0.95) and fewer than hypothetical charge of divalent metal cations. This is a section with predicted ionic nature of metal-ligand in (complexes) coordination compounds. The higher positive charge on Cd compared to Zn reflects lower electronegativity and larger ionic radius of cadmium, contributing to greater transfer of charge from metal to ligands. Higher negative charge on N2 (nitrogen atom that coordinated to metal) in the complex of Cd (-0.39 vs -0.29 for Zn) signifies greater electron donation to the more positively charged (Cd). In Zn complex, sulfur has a negative charge (-0.306), while the Cd complex has a major impact considerably more negative charge (-0.36). This shows clear data of cadmium reality a softer Lewis acid than Zinc, Enhances covalent bonding with sulfur soft donor atom. The NBO charges offer a more profound understanding of the charge transfer from ligands to metal. The total ligand-to-metal charge transfer can be calculated by comparing the formal charges with the NBO charges (Ali et al., 2022). In Zn complex: Total ligand charge ≈ -1.82, indicating significant charge transfer while Cd complex: Total ligand charge ≈ -1.95, showing even greater charge transfer and sulfur charge difference (-0.03 vs -0.36) forecast that Cd has a greater affinity for sulfur donors than Zn (Fig. 14).

Table 6: NBO and charge (e) of ligand and Zn, Cd complexes.

Donor Atom	Ligand	Zn charge	Cd charge
-----	------	0.81782	0.94793
N1	- 0. 27954	-0.2511	-0.27164
		-0.25323	-0.26075
N2	-0.29108	-0.42424	-0.39404
		-0.41468	-0.40928
S*	-0.0341	-0.30631	-0.35684
		-0.3086	-0.32743

* Sulfur atom coordinated to Zn and Cd metals

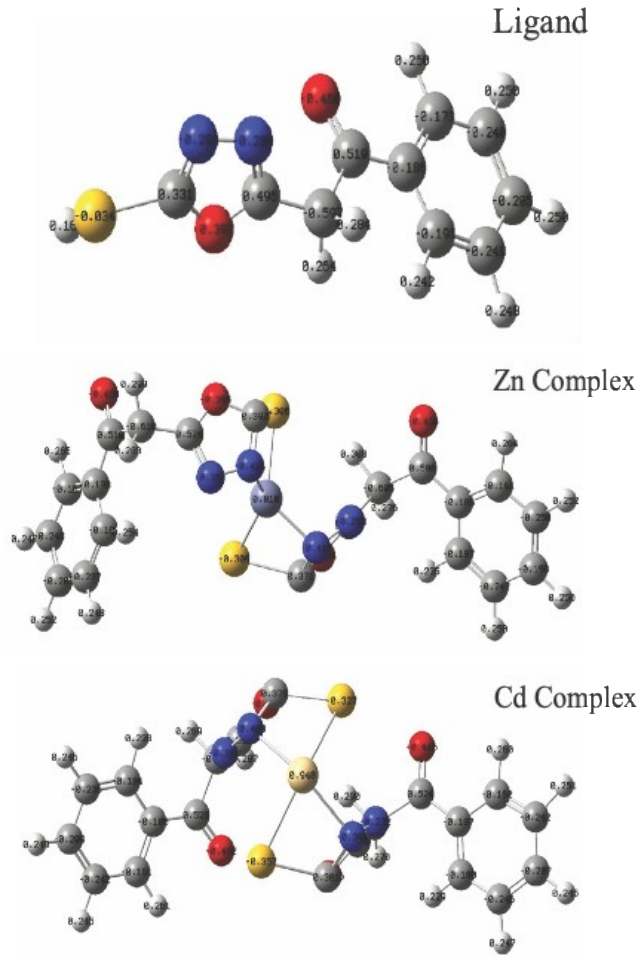

Figure 14. NBO Charge of atoms for Ligand and Zn, Cd complexes.

5. Conclusions

This research successfully synthesized and characterized novel divalent Ni (II), Zn (II), Cd (II), and Hg (II) complexes with a 5-(benzoyl methyl)-1,3,4-oxadiazole-2-thione ligand. Spectroscopic and magnetic data confirmed distorted tetrahedral geometries for the Zn, Cd, and Hg complexes and a distorted square planar structure for the Ni complex. All compounds behaved as non-electrolytes, and elemental analysis verified their proposed stoichiometry.

Evaluation of antioxidant activity revealed that the Zn (II) complex exhibited superior and stable concentration-independent DPPH radical scavenging ability (100% across all concentrations), these data exceeded that of the ascorbic acid standard and the other metal complexes, which exhibited diminished activity at higher concentrations due to comparative instability. The activities of the Ni (II) and Cd (II) complexes decreased at higher concentrations, indicating relative instability.

Computational DFT and NBO analyses provided electronic structure insights, showing a larger HOMO-LUMO energy gap for the Zn complex, correlating with its higher stability. NBO charge calculations indicated significant ligand-to-metal charge transfer, with the Cd complex showing a greater affinity for the sulfur donor. These findings establish a clear link between the structural properties, stability, and bioactivity of the synthesized complexes.

Conflict of interest

The author declares that there is no conflict of interests.

CRediT authorship contribution statement

Bayan Faiq performed the entire research and writing associated with this manuscript.

Acknowledgments

Author is appreciative to the department of chemistry, College of Science, Salahaddin University owned by their cooperation upon finishing this work.

References

Abd El-Nasser, M.G. and Ismail, T.I., (2025). Synthesis, characterization, molecular docking studies, and theoretical calculations of novel Ni (II), Cu (II), and Zn (II) complexes based on benzothiazole derivatives. BMC chemistry, 19(1), pp. 202. https://doi.org/10.1186/s13065-025-01576-1

Abdelrehim, E.S.M., (2021). Synthesis and screening of new [1, 3, 4] oxadiazole, [1, 2, 4] triazole, and [1, 2, 4] triazolo [4, 3-b] [1, 2, 4] triazole derivatives as potential antitumor agents on the colon carcinoma

cell line (HCT-116). ACS omega, 6(2), pp.1687-1696. https://doi.org/10.1021/acsomega.0c05718

Aboraia, A.S., Abdel-Rahman, H.M., Mahfouz, N.M. and El-Gendy, M.A., (2006). Novel 5-(2-hydroxyphenyl)-3-substituted-2, 3-dihydro-1, 3,4-oxadiazole-2-thione derivatives: Promising anticancer agents. Bioorganic & medicinal chemistry, 14(4), pp.1236-1246. https://doi.10.1016/j.bmc.2005.09.053

Akram, M. A., Abdul Rauf, A.R., Aamer Saeed, A.S., Faiz Ahmed, F.A., Sidra Mubeen, S.M., Muhammad Ashraf, M.A., Safdar Hussain, S.H. and Qureshi, A.M., (2018). Synthesis, biological evaluation and molecular docking studies of Mannich bases derived from 1, 3, 4-oxadiazole-2-thiones as potential urease inhibitors. Tropical Journal of Pharmaceutical Research, 17(1), pp127. https://doi.org/10.4314/tjpr.v17i1.18

Ali, K.O., Mohamad, H.A., Gerber, T. and Hosten, E., (2022). Zinc (II) Complex Containing Oxazole Ring: Synthesis, Crystal Structure, Characterization, DFT Calculations, and Hirshfeld Surface Analysis. Acta Chimica Slovenica, 69(4) pp.7682-7690. https://doi.org/10.17344/acsi.2022.7682

AL-Nama, K.S., Saeed, I.A. and Mohammed, A.F., (2025). Synthesis, characterization, DFT, molecular docking, and in vitro screening of metal chelates incorporating Schiff base. Bulletin of the Chemical Society of Ethiopia, 39(4), pp.687-701. https://dx.doi.org/10.4314/bcse.v39i4.7

Al-Wahaibi, L.H., Mohamed, A.A., Tawfik, S.S., Hassan, H.M. and El-Emam, A.A., (2021). 1, 3, 4-Oxadiazole N-Mannich bases: synthesis, antimicrobial, and anti-proliferative activities. Molecules, 26(8), pp.2110. https://doi.org/10.3390/molecules26082110

AYDOĞAN, F., Turgut, Z., Öcal, N. and Erdem, S.S., (2002). Synthesis and electronic structure of new aryl-and alkyl-substituted 1, 3, 4-oxadiazole-2-thione derivatives. Turkish journal of chemistry, 26(2), pp.159-170. https://journals.tubitak.gov.tr/chem

Bala, S., Kamboj, S., Kajal, A., Saini, V. and Prasad, D.N., (2014). 1, 3, 4-oxadiazole derivatives: synthesis, characterization, antimicrobial potential, and computational studies. BioMed research international, 2014(1), pp.172791. http://dx.doi.org/10.1155/2014/172791

Baliyan, S., Mukherjee, R., Priyadarshini, A., Vibhuti, A., Gupta, A., Pandey, R.P. and Chang, C.M., (2022). Determination of antioxidants by DPPH radical scavenging activity and quantitative phytochemical analysis of Ficus religiosa. Molecules, 27(4), pp.1326. https://doi.org/10.3390/molecules27041326

Bharty, M.K., Bharti, A., Dani, R.K., Kushawaha, S.K., Dulare, R. and Singh, N.K., (2012). Studies on novel Cu (II) complexes of 5-(4-hydroxy-phenyl)-1, 3, 4-thiadiazole-2-thiol and 5-thiophen-2-yl-3H-1, 3, 4-oxadiazole-2-thione: Synthesis, spectral and structural characterization. Polyhedron, 41(1), pp.52-60. https://doi.org/10.1016/j.poly.2012.04.025

Bharty, M.K., Dani, R.K., Nath, P., Bharti, A., Singh, N.K., Prakash, O., Singh, R.K. and Butcher, R.J., (2015). Syntheses, structural and thermal studies on Zn (II) complexes of 5-aryl-1, 3, 4-oxadiazole-2-thione and dithiocarbamates: Antibacterial activity and DFT calculations. Polyhedron, 98, pp.84-95. http://dx.doi.org/10.1016/j.poly.2015.05.045

Choudhary, V., Bhatt, A., Dash, D. and Sharma, N., (2019). DFT calculations on molecular structures, HOMO–LUMO study, reactivity descriptors and spectral analyses of newly synthesized diorganotin (IV) 2-chloridophenylacetohydroxamate complexes. Journal of computational chemistry, 40(27), pp.2354-2363. WWW.CHEMISTRYVIEWS.CO

Dani, R.K., Bharty, M.K., Kushawaha, S.K., Prakash, O., Sharma, V.K., Kharwar, R.N., Singh, R.K. and Singh, N.K., (2014). Syntheses, spectral and structural

characterization of trinuclear and mononuclear Zn (II) complexes of N′-benzoyl hydrazine carboperthioate and 5-phenyl-1, 3, 4-oxadiazole-2-thione: An approach to DFT calculation, antibacterial and thermal studies. Polyhedron, 81, pp.261-272. http://dx.doi.org/10.1016/j.poly.2014.06.022

Demir, İ. and İhsan Pekacar, A., (2005). Synthesis and characterization of some nickel (II), cobalt (II), and zinc (II) complexes with Schiff bases derived from the reaction of isonitroso-p-chloroacetophenone and 1,2-diaminoethanewith1,4-diaminobutane. Synthesis and Reactivity in Inorganic, Metal-Organic, and Nano-Metal Chemistry, 35(10), pp.825-828. https://doi.org/10.1080/15533170500358234

Derafa, W., Elkanzi, N.A., Ali, A.M. and Abdou, A., (2024). Three Co (II), Ni (II) and Cu (II) Schiff base complexes incorporating 2-[(4-{[(4-methylphenyl) sulfonothioyl] oxy} phenyl) methylene] amino} benzoic acid: Synthesis, structural, DFT, biological and molecular docking investigation. Bulletin of the Chemical Society of Ethiopia, 38(2), pp.325-346. https://dx.doi.org/10.4314/bcse.v38i2.5

Dhaveethu, K., Ramachandramoorthy, T. and Thirunavukkarasu, K., (2013). Spectroscopic, thermal and biological studies of Zn (II), Cd (II) and Hg (II) complexes derived from 3-aminopyridine and nitrite ion. Journal of the Korean Chemical Society, 57(6), pp.712-720. https://doi.org/10.5012/jkcs.2013.57.6.712

Dilmaghani, K.A. and Ghezelbash, Z.D., (2016). Synthesis of a Series of Novel Tetra-tert-butylcalix [4] arene Linked to 1, 2, 4-Triazole and 1, 3, 4-Oxadiazole Derivatives. Acta Chimica Slovenica, 63(4), pp.790-797. https://doi.org/10.17344/acsi.2016.2637

Faloye, K.O., Tripathi, M.K., Fakola, E.G., Adepiti, A.O., Adesida, S.A., Oyeleke, I.O., Adebayo, P.A., Aregbesola, A.E., Famuyiwa, S.O. and Akinyele, O.F., (2025). Plasmepsin II inhibitory potential of phytochemicals isolated from African antimalarial plants: a computational approach. Journal of Biomolecular Structure and Dynamics, 43(1), pp.505-520. https://doi.org/10.1080/07391102.2023.2283146

Geyl, K.K., Baykova, S.O., Andoskin, P.A., Sharoyko, V.V., Eliseeva, A.A., Baykov, S.V., Semenov, K.N. and Boyarskiy, V.P., (2022). Palladium (II) and Platinum (II) Deprotonated Diaminocarbene Complexes Based on N-(2-Pyridyl) Ureas with Oxadiazole Periphery. Inorganics, 10(12), pp.247. https://doi.org/10.3390/inorganics10120247

Husain, A. and Ajmal, M., (2009). Synthesis of novel 1, 3, 4-oxadiazole derivatives and their biological properties. Acta pharmaceutica, 59(2), pp.223-233. https://doi.org/10.2478/v10007-009-0011-

Kazi, S.A., (2011). Synthesis and Characterization of a New Bidentate Ligand 5-Substituted-(2-methyl-5-nitro-1-imidazomethyl) -1, 3, 4-oxadiazole-2-thione and its Metal Complexes of Ag (I), Cu (II) and Zn (II). Journal of Chemistry, 8, pp. S127-S136. https://doi.org/10.1155/2011/280682

Kurahatti, S., Anchi, A., Rathod, M.R., Pawashe, G.M., Kalkhambkar, R.G. and Kurkuri, M.D., (2025). Ionic liquid-catalyzed, microwave-assisted green synthesis of novel Coumarin-Schiff bases: Characterization, molecular docking, biological and DFT studies. Journal of Molecular Structure, 1324, pp.140853. https://doi.org/10.1016/j.molstruc.2024.140853

Li, Z., Zhan, P. and Liu, X., (2011). 1, 3, 4-Oxadiazole: A privileged structure in antiviral agents. Mini Reviews in Medicinal Chemistry, 11(13), pp.1130-1142. https://doi.org/10.2174/138955711797655407

Mikhailov, I.E., Dushenko, G.A., Gurskii, M.E., Vikrischuk, N.I., Popov, L.D., Revinskii, Y.V., Lyssenko, K.A. and Minkin, V.I., (2019). Synthesis, structure, spectral and luminescence properties

of the tetracoordinated diphenylboron and zinc complexes with 1, 3, 4-oxadiazole and 1, 2, 4-triazole ligands. Polyhedron, 166, pp.73-82. https://doi.org/10.1016/j.poly.2019.03.044

Mohammed, M.Y., Abd, A.N. and Ali, A.S., (2018). Synthesis and Characterization Some of Metals (ll) Complexes' with Mixed Ligands of saccharinate and Isatin Schiff Base. Tikrit Journal of Pure Science, 22(6), pp.56-64. https://doi.org/10.25130/tjps.v22i6.791

Nakamoto, K., (2009). Infrared and Raman spectra of inorganic and coordination compounds, part B: applications in coordination, organometallic, and bioinorganic chemistry. John Wiley & Sons.

Nkungli, N.K., Ghogomu, J.N., Nogheu, L.N. and Gadre, S.R., (2015). DFT and TD-DFT study of Bis [2-(5-Amino-[1,3,4]-oxadiazol-2-yl) Phenol] (Diaqua) M (II) complexes [M= Cu, Ni and Zn]: electronic structures, properties and analyses. Computational Chemistry, 3(3), pp.29-44. http://www.scirp.org/journal/cc

Pandey, R.N., Kumari, G., Nag, A.K. and Gautam, K.V. (2010). MIXED-LIGAND ORGANOMETALLIC COMPLEXES OF RUTHENIUM (II) PALLADIUM (II) AND PLATINUM (II) WITH TRIPHENYL PHOSPHINE AND 2-MERCAPTOBENZOTHIAZOLE. Rasayan J. chem, 3, pp.415-419. http://www.rasayanjournal.com

Pandey, R.N., Nag, A.K., Pande, P. and Singh, S.K., (2010). Spectral studies on cobalt (II) and nickel (II) complexes of bis (1-phenyl tetrazoline)-5, 5'-disulphide. Oriental Journal of Chemistry, 26(1), pp.109. http://creativecommons.org

Prabhu, D.D., Kumar, N.S., Sivadas, A.P., Varghese, S. and Das, S., (2012). Trigonal 1, 3, 4-oxadiazole-based blue emitting liquid crystals and gels. The Journal of Physical Chemistry B, 116(43), pp.13071-13080. https://doi.org/10.1021/jp305349h

Saaid, F.H., Dawood, S.J. and Marbeen, B.H., (2018). Synthesis and Characterization of 1, 3, 4-oxadiazole Derivatives using an Ultrasonic Technique. Al-Mustansiriyah Journal of Science, 29(2), pp.101-105. http://doi.org/10.23851/mjs.v29i2.183

Shaker, S.A.,(2010). Preparation and study of some Mn (II), Co (II), Ni (II), Cu (II), Cd (II) and Pb (II) complexes containing heterocyclic nitrogen donor ligands. Journal of Chemistry, 7(4), pp.1598-1604. http://www.e-journals.net

Silva, F., Veiga, F., Cardoso, C., Dias, F., Cerqueira, F., Medeiros, R. and Paiva-Santos, A.C., (2024). A rapid and simplified DPPH assay for analysis of antioxidant interactions in binary combinations. Microchemical Journal, 202,pp.110801. https://doi.org/10.1016/j.microc.2024.110801

Singh, N.K., Bharty, M.K., Kushawaha, S.K., Dulare, R. and Butcher, R.J., (2010). Manganese (II) complexes of 5-(4-pyridyl), 5-phenyl and 5-(4-methoxy-phenyl)-1,3,4-oxadiazole-2-thione containing2,2′-bipyridyl/etheylenediamine: synthesis, spectral, and X-ray characterization. Transition Metal Chemistry, 35(3), pp.337344. https://doi.org/10.1007/s11243-010-9332-7

Sundaresan, S., Eppelsheimer, J., Carrella, L.M. and Rentschler, E., (2022). Three Novel Thiazole-Arm Containing 1, 3, 4-Oxadiazole-Based [HS-HS] Fe (II) Dinuclear Complexes. Crystals, 12(3), pp.404. https://doi.org/10.3390/cryst12030404

Tang, Y., He, C., Mitchell, L.A., Parrish, D.A. and Shreeve, J.N.M., (2015). Energetic compounds consisting of 1, 2, 5-and 1, 3, 4-oxadiazole rings. Journal of Materials Chemistry A, 3(46), pp.23143-23148. https://doi.org/10.1039/c5ta06898c

Tegegn, D.F., Belachew, H.Z. and Salau, A.O., (2024). DFT/TDDFT calculations of geometry optimization, electronic structure and spectral properties of clevudine and telbivudine for treatment of chronic hepatitis B. Scientific Reports, 14(1), pp.8146. https://doi.org/10.1038/s41598-024-58599-2

Tzanetos, N.P. and Kallitsis, J.K., (2005). Synthesis and optical properties of green-light-emitting

copolymers containing side-chain oxadiazole units. Journal of Polymer Science Part A: Polymer Chemistry, 43(5), pp.1049-1061. https://doi.org/10.1002/pola.20581